Int. J. Solids Structures, 1967, Vol. 3, pp. 413 to 425. Pergamon Press Ltd. Printed in Great Britain

PLASTIC ANALYSIS OF FIBRE-REINFORCED PLATES UNDER ROTATIONALLY SYMMETRIC CONDITIONS

J. ZAWIDZKI and A. SAWCZUK

Polish Academy of Sciences, Warsaw

Abstract—Complete solutions of plastic bending of rotationally symmetric plates are presented in the case of non-homogeneity specific to polar nets of extensible reinforcement. The results are compared with those of homogeneous plates, indicating the differences in collapse loads, collapse modes and stress fields. Optimum design of fibre-reinforced plates is studied.

1. INTRODUCTION

AVAILABLE limit analysis solutions of rotationally symmetric problems of plate flexure concern a wide range of yield criteria [1, 2], material anisotropy [3–5] and piece-wise linear non-homogeneity [6]. However, a technically important case of fibre-reinforced slabs with polar nets has not been studied. Such a type of fibre arrangement results in a special form of non-homogeneity and orthotropy of the plate yield moduli; thus it requires a separate analysis of both the collapse load and the collapse mechanism. This is particularly so because the design based on yield criteria independent of the position co-ordinates, if safe, leads to overestimation of the material required.

This note stems from the study of reinforced concrete plates with non-uniform reinforcement. The elastic–plastic flexure of such structures was studied by Olszak and Murzewski [7]. Attention was confined rather to the initial stages of elastic–plastic bending with account for both the non-homogeneity and orthotropy. In the present paper complete solutions to the plastic bending of circular and annular plates are presented in case of nonhomogeneity specific to polar nets of extensible reinforcement. The results are compared with those of homogeneous plates, indicating the differences in collapse modes and stress fields. Suggestions regarding the optimum plastic design of the considered structures are given.

2. ASSUMPTIONS

We consider plates made of perfectly plastic material supporting compression only and reinforced with perfectly plastic fibres to carry tension. The response of such structures to external loads is studied under the following specific assumptions:

(a) the rigid–plastic model of deformation applies.

(b) the place is plastically orthotropic and non-homogeneous and with respect to both of these properties the structure is rotationally symmetric,

(c) the maximum principal moment yield criterion applies,

(d) the stress field is related to the rates of deformation through the plastic potential flow law.

We are interested in complete solutions of the plastic plate problem, thus we are required

(a) to determine the plastic and rigid zones,

(b) to find the collapse load,

(c) to ascertain a statically admissible stress field satisfying the actual yield condition in the deforming zones and not violating this condition in the rigid ones,

(d) to associate with the stress solution a kinematically admissible collapse mode assuring a positive dissipation in the deforming zones.

We purposely adopt a procedure leading to the complete solution, without using the theorems of limit analysis.

Let us consider a circular slab of radius R reinforced with a polar net, the pole coinciding with the plate centre. The circumferential reinforcement is uniform, thus the circumferential yield moments do not depend upon the position. The radial reinforcement is uniform per unit angle, thus the radial yield moment is inversely proportional to the radius. Reinforcement consists of different nets for positive and negative bending, therefore different yield moments result for positive and negative bending. The yield moments of such orthotropic and non-homogeneous structures are shown in Fig. 1, which indicates also the adopted notation and sign convention.

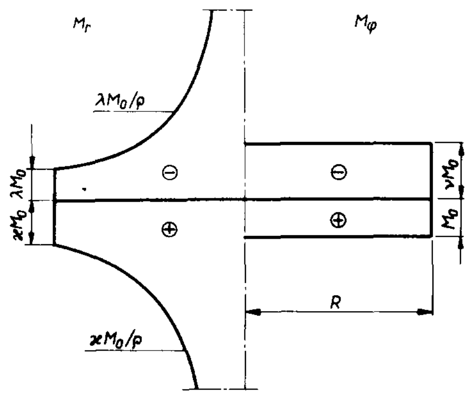

FIG. 1. Variation of yield moments with radius.

The following dimensionless variables will be used

$$\varrho = \frac{r}{R}, \qquad m = \frac{M}{M_0}, \qquad q = \frac{QR}{M_0}, \qquad P = \frac{pR^2}{M_0}, \qquad w = \frac{W}{R}, \tag{1}$$

where M, Q, p and W stand for the bending moments, the shear force, the external loading and the deflection rate (positive downwards), respectively. The appropriate dimensionless form of the non-homogeneous yield equation is

$$f_1 = m_r - \varkappa/\varrho = 0 \quad \text{or} \quad f_3 = m_r + \lambda/\varrho = 0 \quad \text{for} \quad -\nu \le m_\varphi \le 1, \varrho > \varepsilon \to 0, \tag{2}$$

$$f_2 = m_\varphi - 1 = 0 \quad \text{or} \quad f_4 = m_\varphi + \nu = 0 \quad \text{for} \quad -\lambda/\varrho \le m_r \le \varkappa/\varrho, \tag{3}$$

In view of (1) the differential equilibrium equations become

$$(\varrho m_r)' - m_\varphi - \varrho q = 0, \qquad (\varrho q)' + \varrho P = 0. \tag{4}$$

Stress fields in plastic bending can have discontinuities. Under the requirements $m_r^+(\varrho)-m_r^-(\varrho) \equiv m_r] = 0$ and $P] = 0$ the equations (4) yield the following relation on a circumferential line of stress discontinuity

$$\varrho m_r'] - m_\varphi] = 0 \tag{5}$$

The plastic potential flow law applied to the yield equations (2) and (3) and combined with the deflection–curvature relations of the plate theory gives the following expressions for the rates of curvature

$$\frac{\varrho w''}{w'} = \frac{\partial f_\alpha/\partial m_r}{\partial f_\alpha/\partial m_\varphi} = \begin{cases} \infty, & \alpha = 1, 3 \\ 0, & \alpha = 2, 4 \end{cases} \tag{6}$$

Thus the displacement rate field is not influenced by the non-homogeneity in question and collapse mechanisms consist of surfaces

$$w = c_1 = \text{const.} \quad \text{for} \quad f_1 = 0, \quad f_3 = 0, \tag{7}$$

$$w = c_2\varrho + c_3 \quad \text{for} \quad f_2 = 0, \quad f_4 = 0, \tag{8}$$

as they are for homogeneous plates under the maximum moment yield criterion [2]. The hinge line forms whenever $f_1 = f_2, f_1 = f_4, f_3 = f_2, f_3 = f_4$, i.e., at the corners of the yield rectangle defined by (2) and (3) for a fixed ϱ.

3. CIRCULAR PLATES

In order to contrast the behaviour of the studied slabs and of homogeneous plates, let us consider a clamped circular plate subjected to uniform pressure p for $\varepsilon \le \varrho \le 1$. Since the problem is statically determinate with respect to the shear force equations (4) reduce to

$$(\varrho m_r)' - m_\varphi + P\varrho^2/2 = 0. \tag{9}$$

One can conclude from (7) and (8) that the most general form of collapse is associated with plastic deformation confined to the annular region $\varrho_0 \le \varrho \le 1$ with the central part remaining rigid. Therefore in the deforming region the stress profile corresponds to $f_2 = 0$, i.e.

$$m_\varphi(\varrho) = 1, \quad -\lambda/\varrho \le m_r(\varrho) \le \varkappa/\varrho, \quad \varrho_0 \le \varrho \le 1, \tag{10}$$

the stress boundary conditions being

$$m_r(1) = -\lambda, \quad m_r(\varrho_0) = \varkappa/\varrho_0. \tag{11}$$

Integration of (9) for the yield equation (10) gives

$$m_r = 1 - P\varrho^2 + A/\varrho. \tag{12}$$

For evaluation of the collapse load, the radius ϱ_0 and the integration constant A we have only two conditions (11). However, if we want to extend the stress field into the rigid region $\langle 0, \varrho_0 \rangle$ an additional relation can be established. Looking for a continuous extension with regard to m_φ, thus requiring $m_\varphi] = 0$, the relation (5) results in the following condition at the rigid–plastic boundary

$$m_r'] = 0 \quad \text{for} \quad \varrho = \varrho_0 \tag{13}$$

At $\varrho = \varrho_0$ the m_r satisfies (10) and in the neighbourhood it is required not to violate the yield condition; thus it has to satisfy the condition $m_r(\varrho) \leq \varkappa/\varrho$. This, in view of (11) and (13), results in the requirement for m_r to be tangent to the yield function defining the non-homogeneity, thus

$$m'_r|_{\varrho=\varrho_0} = -\varkappa/\varrho_0^2. \tag{14}$$

The conditions (11) and (14) constitute a complete set for the unknown quantities and completely specify the "static" problem without any reference to the theorems on bounds and without any reference to the kinematics. Considering simply kinematics and making use of the upper bound theorem we would be able to derive (15) below but this would leave us without sufficient information concerning the stress field in the central (rigid) zone. Eventually, for the radius of the rigid–plastic boundary the following equation is obtained

$$2\varrho_0^3 - 3(1+\varkappa+\lambda)\varrho_0^2 + 1 = 0. \tag{15}$$

It can be demonstrated that (15) has only one real root in $\langle 0, 1 \rangle$.

The collapse load for the stress profile specified by (10) and (11) becomes

$$P = 2/\varrho_0^2, \tag{16}$$

ϱ_0 being the root of (15), whereas the integration constant appearing in (12) is $A = \frac{1}{3}\varrho_0^2 - (1+\lambda)$.

To establish the range of validity of the solution (16) it is necessary to find an extension of the stress field from the plastic region into the central rigid zone. We are looking for an extension satisfying the following continuity conditions on the rigid plastic boundary

$$m_r(\varrho_0) = \varkappa/\varrho_0, \qquad m_\varphi(\varrho_0) = 1 \quad \text{or} \quad m'_r(\varrho_0) = -\varkappa/\varrho_0^2, \tag{17}$$

Moreover we require

$$m_r(0) = m_\varphi(0), \qquad m_\varphi(0) \leq 1 \tag{18}$$

The simplest possible polynomial extension satisfying (17) and (18) has the form

$$m_r = A_1 + A_2\varrho^2 + A_3\varrho^3, \qquad m_\varphi = A_1 + (3A_2\varrho_0^2 + 1)\varrho^2/\varrho_0^2 + 4A_3\varrho^3 \tag{19}$$

if the equations (9) and (16) have to be satisfied. Constants appearing in (19) are determined from the conditions (17) and (18). The stress field in the plate is

$$m_r = \begin{cases} \dfrac{6\varkappa - \varrho_0}{3\varrho_0} + \dfrac{\varrho_0 - 2\varkappa}{\varrho_0}\left(\dfrac{\varrho}{\varrho_0}\right)^2 - \dfrac{2\varrho_0 - 3\varkappa}{3\varrho_0}\left(\dfrac{\varrho}{\varrho_0}\right)^3, & 0 \leq \varrho \leq \varrho_0, \quad (20) \\ 1 - \dfrac{3(1+\lambda)\varrho_0^2 - 1}{3\varrho_0^3}\left(\dfrac{\varrho}{\varrho_0}\right)^{-1} - \dfrac{1}{3}\left(\dfrac{\varrho}{\varrho_0}\right)^2, & \varrho_0 \leq \varrho \leq 1, \quad (21) \end{cases}$$

$$m_\varphi = \begin{cases} \dfrac{6\varkappa - \varrho_0}{3\varrho_0} + 2\dfrac{2\varrho_0 - 3\varkappa}{\varrho_0}\left(\dfrac{\varrho}{\varrho_0}\right)^2 - 4\dfrac{2\varrho_0 - 3\varkappa}{\varrho_0}\left(\dfrac{\varrho}{\varrho_0}\right)^3, & 0 \leq \varrho \leq \varrho_0, \quad (22) \\ 1, & \varrho_0 \leq \varrho \leq 1, \quad (23) \end{cases}$$

where ϱ_0 is the root of (15). Now it remains only to check whether the stresses (20) and (22) remain within the yield surface, thus whether

$$m_r(\varrho) \leq \varkappa/\varrho, \qquad m_\varphi(\varrho) \leq 1 \quad \text{for} \quad 0 \leq \varrho \leq \varrho_0 \tag{24}$$

The first of inequalities (24) is easily seen to be satisfied because

$$\frac{\varkappa}{\varrho}-m_r = \frac{\varkappa}{\varrho}\left[1-\left(\frac{\varrho}{\varrho_0}\right)^2\right]\left\{\left[1-\left(\frac{\varrho}{\varrho_0}\right)^2\right]+\frac{1}{3}\left(\frac{\varrho}{\varrho_0}\right)\left[1+2\left(\frac{\varrho}{\varrho_0}\right)\right]\right\} \geq 0. \tag{25}$$

To check whether the circumferential moment (22) remains admissible we observe that $m_\varphi(0) = (6\varkappa-\varrho_0)/3\varrho_0 \leq 1$ holds, provided that $2\varrho_0 \geq 3\varkappa$. Moreover $m_\varphi(\varrho_0) = 1$. To prove the second of (24), therefore, it is sufficient to show that m_φ is not a decreasing function within the considered region, thus

$$m'_\varphi \geq 0 \quad \text{for} \quad 0 \leq \varrho \leq \varrho_0. \tag{26}$$

In fact, performing the prescribed differentiation we obtain

$$m'_\varphi = 4\frac{2\varrho_0-3\varkappa}{\varrho_0^2}\left(\frac{\varrho}{\varrho_0}\right)\left[1-\left(\frac{\varrho}{\varrho_0}\right)\right] \geq 0 \quad \text{for} \quad 0 \leq \varrho \leq \varrho_0, \tag{27}$$

which supplies the proof, provided that

$$2\varrho_0-3\varkappa \geq 0. \tag{28}$$

The relation (28) appears to have a simple justification. If the yield equation $m_\varphi = 1$ is assumed to hold for the entire plate, the appropriate stress boundary conditions, in view of (18), are $m_r(1) = -\lambda$, $m_r(0) = 1$. Therefore the equation (12), together with the above two boundary conditions, yields the collapse load,

$$P = 6(1+\lambda) \tag{29}$$

and the stress field

$$m_\varphi = 1, \qquad m_r = 1-(1+\lambda)\varrho^2. \tag{30}$$

The collapse load (16) cannot exceed the value (29) which is associated with the total collapse. Thus

$$\varrho_0 \geq \varrho_0^* \equiv [3(1+\lambda)]^{-\frac{1}{2}} \tag{31}$$

and therefore the solution (16) holds for

$$\varkappa \leq \varkappa^* \equiv \frac{2}{3\sqrt{[3(1+\lambda)]}} = \tfrac{2}{3}\varrho_0^*, \tag{32}$$

as obtained from (15).

The relations (31) and (32), however, lead to the requirement $3\varkappa \leq 2\varrho_0$, thus precisely to that given by (29). The critical relation (32) is shown in Fig. 2.

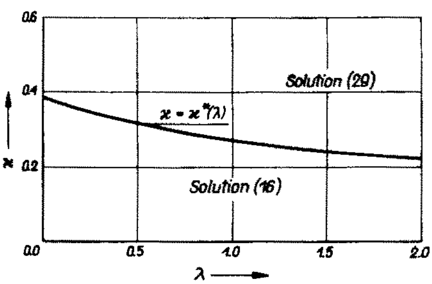

FIG. 2. Domains of validity of solutions for circular plates.

It can be easily verified that for $\varrho_0 \to \varrho_0^*$ the stress equations (20)–(23) pass into (30). Thus there is a continuous transition to the stress field of a homogeneous plate. For a specific case of $\lambda = 0$ in (11), thus for a simply supported plate in Fig. 3(a) the collapse load is plotted versus the amount of reinforcement in the circumferential direction at the plate boundary. The position of the rigid–plastic boundary is shown in Fig. 3(b). It is seen from these figures that the plastic non-homogeneity has both qualitative and quantitative influence on the behaviour of plastic plates.

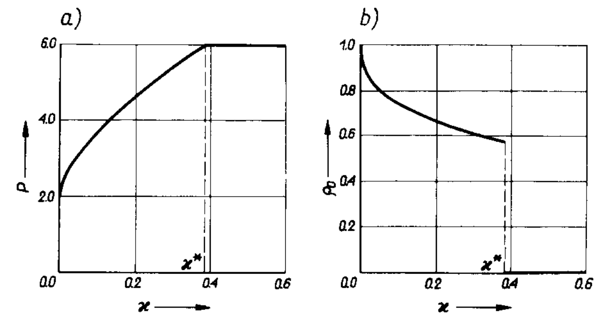

FIG. 3. Collapse load and radius of the rigid zone vs. density of the radial reinforcement.

The presented solutions are complete because displacement rate fields associated with the collapse loads are easily found from (7) and (8). We have

$$w = w_0 \begin{cases} 1, & 0 \le \varrho \le \varrho_0, \quad (33) \\ (1-\varrho)/(1-\varrho_0), & \varrho_0 \le \varrho \le 1, \quad (34) \end{cases}$$

if $\varkappa \le 2\varrho_0^*/3$ and

$$w = w_0(1-\varrho), \qquad 0 \le \varrho \le 1, \tag{35}$$

otherwise, w_0 being the undetermined reference rate of deflection. These collapse modes assure positiveness of the internal dissipation, the checking procedure being trivial.

For the sake of illustration, the stress field of the complete solution for a particular case of a clamped plate is given in Fig. 4. The broken lines represent the yield moments,

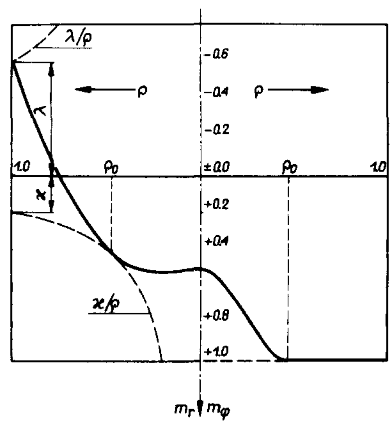

FIG. 4. Stress field of the complete solution.

the heavy ones the actual distribution of bending moments for $\lambda = 0{\cdot}6$, $\varkappa = 0{\cdot}2 < \varkappa^* = 0{\cdot}304$. In this case $\varrho_0 = 0{\cdot}474$, and therefore the collapse mode is a truncated cone as defined by (33) and (34).

The fact that for $\varkappa \geq \varkappa^*$ the intensity of the radial reinforcement does not influence the collapse load provides hints for the rational design of fibre-reinforced plates.

4. ANNULAR PLATES

Extension of the proceding analysis to annular plates with one edge free is almost trivial and will not be discussed here. We consider an annulus of radii R and αR, $\alpha < 1$, supported at both boundaries and subjected to uniformly distributed pressure p. The yield condition of Fig. 1 applies, except possibly for an additional radial reinforcement at the outer support such that $\mu > \lambda$ for $\beta \leq \varrho \leq 1$. This additional reinforcement is applied in a narrow region at the boundary and it is justified by requirements of the rational design.

In annular plates at collapse the stress profile passes through three different regimes. This is required by the associated flow law in conjunction with the conditions of kinematical admissibility of a collapse mode (cf. [8, 2]). In the considered case the set of yield equations is

$$m_\varphi = -\nu, \qquad -\lambda/\varrho \leq m_r \leq \varkappa/\varrho, \qquad \alpha \leq \varrho \leq \varrho_1, \tag{36}$$

$$m_r = \varkappa/\varrho, \qquad -\nu \leq m_\varphi \leq 1, \qquad \varrho_1 \leq \varrho \leq \varrho_2, \tag{37}$$

$$m_\varphi = 1, \quad \begin{cases} -\lambda/\varrho \leq m_r \leq \varkappa/\varrho, & \varrho_2 \leq \varrho \leq \beta, \quad (38) \\ -\mu/\varrho \leq m_r \leq -\lambda/\varrho, & \beta \leq \varrho \leq 1. \quad (39) \end{cases}$$

In view of the general solution (7) and (8) for the collapse mode these yield equations are associated with the following collapse mechanism

$$\frac{w}{w_0} = \begin{cases} (\varrho-\alpha)/(\varrho_1-\alpha), & \alpha \leq \varrho \leq \varrho_1, \quad (40) \\ 1, & \varrho_1 \leq \varrho \leq \varrho_2, \quad (41) \\ (1-\varrho)/(1-\varrho_2), & \varrho_2 \leq \varrho \leq 1, \quad (42) \end{cases}$$

which is quite analogous to that of a homogeneous plate, except, possibly, for the different values of the parameters.

The above relations indicate the physical meaning of the stress profile transition radii ϱ_1 and ϱ_2, such that

$$\alpha < \varrho_1 < \varrho_2 < \beta < 1.$$

Annular plates constitute a statically indeterminate problem with respect to the shear and the second of equations (4) yields the expression

$$q = -P\varrho/2 + A/\varrho, \tag{43}$$

where A is a constant of integration common for all regimes (36) to (39). In view of (43) the first of (4) takes the form

$$(\varrho m_r)' = m_\varphi - P\varrho^2/2 + A \tag{44}$$

and has to be integrated for the actual stress profiles. The resulting stress equations are

$$m_r = -\nu - P\varrho^2/6 + A + C/\varrho, \qquad m_\varphi = -\nu, \qquad \alpha \leq \varrho \leq \varrho_1, \tag{45}$$

$$m_r = \varkappa/\varrho, \qquad m_\varphi = P\varrho^2/2 - A, \qquad \varrho_1 \leq \varrho \leq \varrho_2, \tag{46}$$

$$m_r = 1 - P\varrho^2/6 + A + B/\varrho, \qquad m_\varphi = 1, \qquad \varrho_2 \leq \varrho \leq 1. \tag{47}$$

In comparison with a homogeneous plate, only the relations (46) differ, because m_r is no longer constant.

To find the unknown parameters ϱ_1 and ϱ_2, the collapse load P and the integration constants A, B, C, we have the following stress boundary conditions

$$m_r(\alpha) = -\lambda/\alpha, \qquad m_r(1) = -\mu \tag{48}$$

The remaining relations are supplied by the continuity requirements

$$m_r] = 0, \qquad m_\varphi] = 0 \quad \text{for} \quad \varrho = \varrho_1 \quad \text{and} \quad \varrho = \varrho_2. \tag{49}$$

Solving these equations, one obtains the collapse load

$$\frac{P}{1+\nu} = \frac{2}{\varrho_2^2 - \varrho_1^2} \tag{50}$$

and the following system for the parameters

$$\left.\begin{aligned} \alpha^3 + 2\varrho_1^3 - 3(\alpha - \Lambda)\varrho_1^2 - 3\Lambda\varrho_2^2 = 0 \\ 1 + 3\Omega\varrho_1^2 + 2\varrho_2^3 - 3(1+\Omega)\varrho_2^2 = 0 \end{aligned}\right\}, \tag{51}$$

where

$$\Lambda = (\varkappa + \lambda)/(1+\nu), \qquad \Omega = (\varkappa + \mu)/(1+\nu). \tag{52}$$

The stress equations are

$$m_r = \left\{\begin{array}{ll} \frac{P}{2}\left\{\varrho_1^2 + \left[\frac{\varkappa}{1+\nu}(\varrho_2^2 - \varrho_1^2) - \frac{2}{3}\varrho_1^3\right]\frac{1}{\varrho} - \frac{1}{3}\varrho^2\right\}, & \alpha \le \varrho \le \varrho_1, \\ \varkappa/\varrho, & \varrho_1 \le \varrho \le \varrho_2, \\ \frac{P}{2}\left\{\varrho_2^2 + \left[\frac{\varkappa}{1+\nu}(\varrho_2^2 - \varrho_1^2) - \frac{2}{3}\varrho_2^3\right]\frac{1}{\varrho} - \frac{1}{3}\varrho^2\right\}, & \varrho_2 \le \varrho \le 1, \end{array}\right\} \tag{53}$$

$$m_\varphi = \left\{\begin{array}{ll} -\nu & \alpha \le \varrho \le \varrho_1, \\ 1 - \frac{P}{2}(\varrho_2^2 - \varrho_1^2) & \varrho_1 \le \varrho \le \varrho_2, \\ 1 & \varrho_2 \le \varrho \le 1. \end{array}\right\} \tag{54}$$

The total reaction at the inner support is

$$S = \pi M_0[P(\varrho_1^2 - \alpha^2) + 2\nu]. \tag{55}$$

The solution presented is complete because it is both statically and kinematically admissible and satisfies the requirement of positiveness of the internal dissipation. This last condition can easily be checked, comparing the signs of curvatures of the deflection rate (40)–(42) with the signs of the moments (54).

An example of the resulting stress profile is shown in Fig. 5 by the abcd line. It corresponds to the case of $\alpha = 0{\cdot}2$, $\Lambda = 0{\cdot}6$, $\Omega = 0{\cdot}8$. For the sake of clarity this stress profile has been drawn on the yield surface, as represented in the space of $(m_r, m_\varphi, \varrho)$ (cf [6]). In comparison with the homogeneous case the stress field in the region $\varrho_1 \le \varrho \le \varrho_2$ differs considerably, since $m_r =$ const. no longer holds.

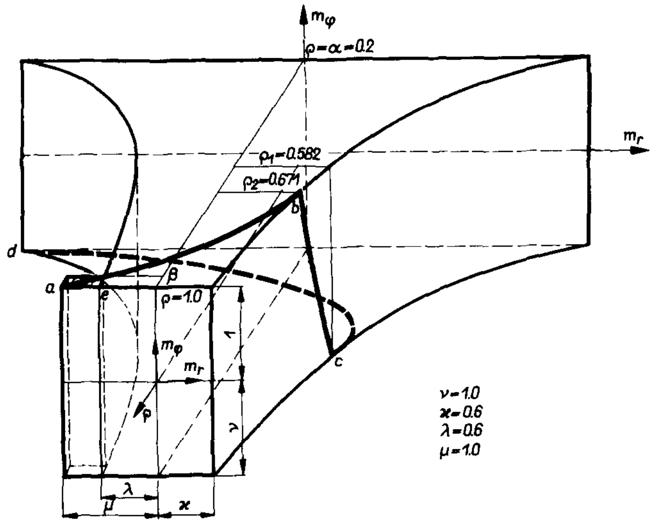

FIG. 5. Stress profile for annular plates.

If the reinforcing net is made stronger at the outer support (as indicated by the a–e line in Fig. 5), the necessary extension $1-\beta$ of the reinforcement in the field follows from the requirement $m_r(\beta) = -\lambda/\beta$. This yields the equation $\beta^3-3\varrho_2^2\beta-3\Lambda(\varrho_2^2-\varrho_1^2)+2\varrho_2^3 = 0$. In case of reinforced concrete plates the additional net extends deeper into the field in order to assure the necessary bond force at $\varrho = \beta$.

It is seen from (51) that the solutions depend upon combinations of the characteristic yield properties of the top and bottom nets. For the case $\Lambda = \Omega$, which includes among others also the case of simply supported plates, the values of ϱ_1 and ϱ_2 are plotted in Figs. 6 and 7. The broken lines in Fig. 7 correspond to solutions for homogeneous plates of the

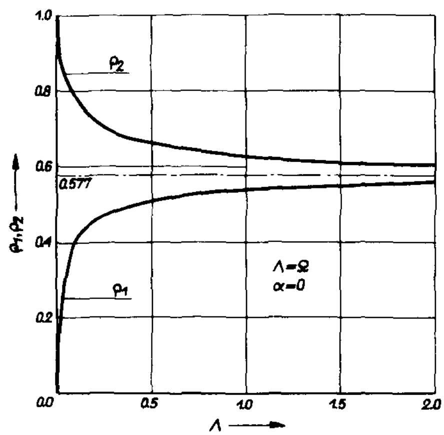

FIG. 6. Radii of the rigid zone in annular plates.

same geometry. Since the collapse load for homogeneous plates is given by relation (50), the differences in the values of ϱ_1 and ϱ_2 indicate differences in the collapse load.

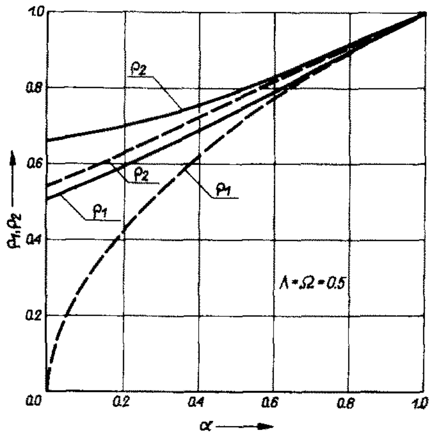

FIG. 7. Comparison of the collapse modes for isotropic and radially reinforced plates.

It is clear from Fig. 7 that the polar net changes considerably the parameters of the yield mechanism. Moreover, in a homogeneous point-supported plate ($\alpha = 0$) a singularity in the stress field takes place, $m_\varphi(0)] = 2$.

In Fig. 8 the collapse load versus the characteristic parameter $\Lambda = \Omega$ is plotted for two values of the internal support diameter. Numerical data regarding the cases considered

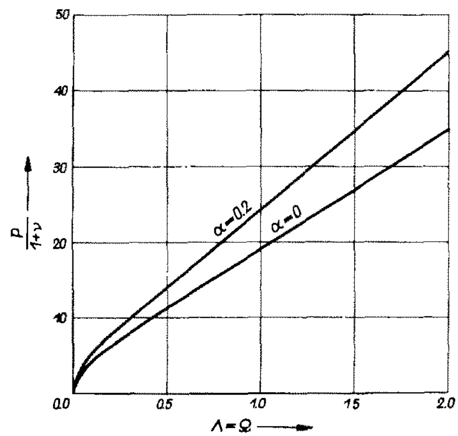

FIG. 8. Collapse loads for annular ($\alpha = 0{\cdot}2$) and point supported ($\alpha = 0$) plates.

are summarized in Table 1. In Fig. 9 a comparison of the collapse loads for annular homogeneous (square mesh) and non-homogeneous (polar net) plates is presented. It is seen that considerable differences in numerical values exist.

It is worthwhile to mention that for annular plates the necessity of introducing a critical value of orthotropy, analogous to that given by (32), does not arise and (50) is generally valid.

TABLE 1

$\Lambda = \Omega$	$\alpha = 0{\cdot}0$			$\alpha = 0{\cdot}2$		
	ϱ_1	ϱ_2	$\frac{P}{1+\nu}$	ϱ_1	ϱ_2	$\frac{P}{1+\nu}$
0·0	0·0000	1·0000	0·000	0·0000	1·0000	0·000
0·1	0·4028	0·7734	4·598	0·5031	0·7917	5·353
0·2	0·4551	0·7222	6·361	0·5478	0·7494	7·645
0·5	0·5105	0·6617	11·284	0·5924	0·7022	14·071
1·0	0·5386	0·6279	19·201	0·6142	0·6774	24·498
2·0	0·5561	0·6055	34·855	0·6274	0·6618	45·086
∞	0·5774	0·5774	∞	0·6429	0·6429	∞

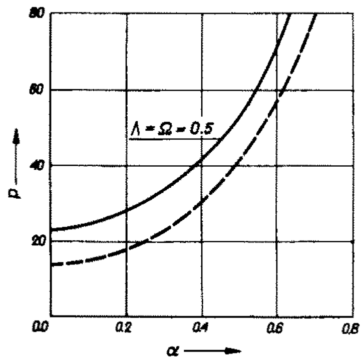

FIG. 9. Comparison of the collapse loads for isotropic and fibre reinforced plates.

5. OPTIMUM DESIGN

From the limit analysis of plates reinforced with polar nets there follows certain consequences regarding the design. Assuming the volume of reinforcement to be the characteristic of an optimum design, we analyse the problem with the example of simply supported plates.

Consider an annular plate as in Section 4, with equal nets for positive and negative bending, thus $\nu = 1$. The volume of the circumferential and the radial reinforcement is, respectively,

$$V_\varphi = \gamma M_0 \pi R^2 (1-\alpha^2), \qquad V_r = 2\gamma\varkappa M_0 \pi R^2 (1-\alpha), \tag{56}$$

where γ stands for the constant depending upon the yield point of reinforcement and upon the lever of internal forces. The total volume can be expressed as follows

$$V = \pi p \gamma (1-\alpha) R^4 \,.\, \Phi, \tag{57}$$

where the function to be minimized is

$$\Phi = (1+\alpha+2\varkappa)/P, \tag{58}$$

P being the dimensionless load.

Let us consider a circular plate. Then $\alpha = 0$ and in view of (16) and (29) one obtains

$$\Phi = \begin{cases} \frac{1}{2}(1+2\varkappa)\varrho_0^2, & \varkappa \leq \varkappa^*, \quad (59) \\ \frac{1}{6}(1+2\varkappa), & \varkappa \geq \varkappa^*. \quad (60) \end{cases}$$

Since $\varrho_0 = \varrho_0(\varkappa)$ is given by (15), these relations can be expressed in terms of $\varkappa$ only. This is shown in Fig. 10. The minimum of Φ with respect to $\varkappa$ is obtained for $\varkappa_e = \varkappa^* = 0{\cdot}385$, the collapse load being as given by (16), and equal to that given by (29).

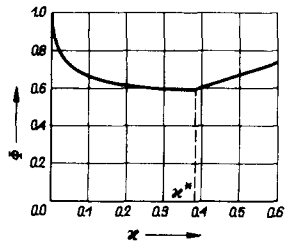

FIG. 10. Optimum design arrangement of reinforcement for circular plates.

If the plate were isotropic, the volume of reinforcement would be related to the yield moment $\overline{M}_0$ and to the loading $\bar{p}$ as follows

$$V = 2\gamma\overline{M}_0\pi R^2 = \tfrac{1}{3}\pi\bar{p}\gamma R^4. \tag{61}$$

From comparison of (61) with the value given by (57) for $\varkappa = \varkappa_e$, we obtain

$$p = \frac{2}{1+2\varkappa^*}\bar{p} = 1{\cdot}13\bar{p}. \tag{62}$$

For an annular plate the function (58) takes the form

$$\Phi = \tfrac{1}{4}(1+\alpha+2\varkappa)(\varrho_2^2-\varrho_1^2), \tag{63}$$

the functions $\varrho_1(\varkappa)$ and $\varrho_2(\varkappa)$ being defined by (51). In Fig. 11 the resulting diagrams are shown for two cases of the inner radius. It is seen from this figure that the optimum design is not sensitive to $\varkappa$ in the large range of $\varkappa \geq \sim 1$.

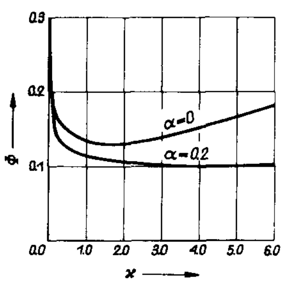

FIG. 11. Optimum design arrangement of reinforcement for annular plates.

The carrying capacity of a homogeneous plate for $\alpha = 0$ is $\bar{p}R^2/\bar{M}_0 = 13{\cdot}72$, [5], and the total volume of reinforcement in this case is

$$V = 2\gamma\bar{M}_0\pi R^2 = \frac{2}{13{\cdot}72}\pi\bar{p}\gamma R^2. \tag{64}$$

Comparing this value with (57) for $\alpha = 0$ and $\varkappa = 2 \approx \varkappa_e$ one finds that a non-homogeneous plate of properly arranged reinforcement carries the load

$$p = \frac{2}{13{\cdot}72}\frac{1}{\Phi(2)}\bar{p} = 1{\cdot}12\bar{p}. \tag{65}$$

The results (62) and (65) demonstrate that non-homogeneous plates of the non-homogeneity produced by the polar nets of reinforcement can be designed to carry higher loads than homogeneous plates. This fact, together with the results concerning stress fields and collapse modes, indicates the technical aspects of the studied problem. The yield line theory [9, 2], can be easily adjusted to cover this type of non-homogeneity.

REFERENCES

[1] P. G. Hodge, *Limit Analysis of Rotationally Symmetric Plates and Shells*. Prentice Hall (1963).
[2] A. Sawczuk and Th. Jaeger, *Grenztragfähigkeits-Theorie der Platten*. Springer (1963).
[3] A. Sawczuk, *Archwm. Mech. stosow.* **8**, 549 (1956).
[4] D. Niepostyn, *Nośność graniczna płyt kołowo-symetrycznych*. Arkady, Warsaw (1963).
[5] J. Markowitz, Ling-Wen Hu, Plastic analysis of orthotropic circular plates, *J. Engng Mech. Div., Proc. ASCE*, **90**, 251 (1964).
[6] J. A. König, J. Rychlewski, *Int. J. Solids Struct.* **2**, 493 (1966).
[7] W. Olszak, J. Murzewski, *Archwm. Mech. stosow.* **9**, 467, 605 (1957).
[8] Z. Mróz, A. Sawczuk, *Izv. AN SSSR, Otd Tech. Nauk. Mekh. i Mashinostr.* **2**, 127 (1959).
[9] K. W. Johansen, Yield line theory. *Cem. Concr. Ass.* (1962).

(*Received* 28 *February* 1966; *revised* 24 *June* 1966)

Résumé—Des solutions complètes de flexion plastique de plaques rotationnelles symmétriques sont présentées dans le cas de non-homogénéité spécifique à des réseaux polaires de renforcement extensible. Les résultats sont comparés à ceux de plaques homogènes, indiquant la différence en capacités portantes et mécanismes de rupture ainsi qu'en distribution de contraintes. Un projet optimum pour plaques de béton armé est étudié.

Zusammenfassung—Vollständige Lösungen werden gegeben für die plastische Verbiegung rotationssymmetrischer Platten im Falle der Ungleichförmigkeit die Polarnetzen mit ausdehnbarer Bewehrung eigen ist. Die Resultate werden mit denen homogener Platten verglichen und die Unterschiede der Bruchlasten, der Durchbiegungsgeschwindigkeiten und der Spannungfelder werden gezeigt. Der optimale Entwurf für Bewehrte Platten wird untersucht.

Абстракт—Предлагаются полные решения пластического изгиба вращательно симметрических пластин в случае неоднородности, специфической для полярных сеток армиробания. Результаты сравниваются с результатами однородной пластины, указывая разницу в разрушающих нагрузках, механизмах разрумения и полях напряжения. Изучается гроблема мини-маьного арииробания железобегонных пластин.